

Prediction of switchable half semiconductor in d^1 transition metal dichalcogenide monolayers

Peng-Ru Huang and Yao He*

Department of Physics, Yunnan University, Kunming 650091, China

Hridis K. Pal and Markus Kindermann

School of Physics, Georgia Institute of Technology, Atlanta, Georgia 30332, USA

We propose that a half semiconducting state can exist in trigonal-prismatic transition metal dichalcogenide (TMDC) monolayers of d^1 configuration. In that state both electrons and holes are spin polarized and share the same spin channel. On the basis of hybrid density functional theory, we predict in particular that VS_2 monolayers are half semiconductors with a direct band gap. Moreover, we find that the conduction electron spin orientation of VS_2 switches under moderate strain. Our predictions thus open up intriguing possibilities for applications of VS_2 in spintronics and optoelectronics. Our analysis of trigonal-prismatic group-V MX_2 ($M=V, Nb, Ta$; $X=S, Se, Te$) monolayers reveals a broad diversity of electronic states that can be understood qualitatively in terms of localization of d electrons.

PACS numbers: 73.20.At,73.22.-f,75.30.-m

Two-dimensional transition metal dichalcogenides (TMDCs) have been the subject of intense research over the past decade because of their unusual electronic properties and potential applications in future nanoelectronic devices [1–3]. The prototype of such materials is MoS_2 , which undergoes a transition from an indirect band gap in the bulk to a direct band gap in the monolayer [4]. The direct-band-gap transition, together with its valley and spin selective properties, makes the material very promising for new generation electronics [5, 6]. Related properties were also observed in other group-VI dichalcogenides such as $MoSe_2$, WS_2 and WSe_2 [7–9]. In comparison, the central topic in group-V TMDCs is electronic instabilities [10–12]. Owing to complicated electron-electron and electron-phonon interactions, this series of compounds displays a rich phase diagram which includes metal, charge density wave (CDW), Mott insulator, and even superconductor [13]. In addition, their electronic structure appears to be highly sensitive to temperature and pressure, which can induce CDW or metal-insulator transitions [14]. The complexity of the electronic structure of these materials holds promise of more surprising physics yet to be discovered.

In this Letter, we study the electronic structures of trigonal-prismatic MX_2 ($M=V, Nb, Ta$; $X=S, Se, Te$) monolayers based on first-principle calculations at the level of the hybrid functional, and propose that the ground state of VS_2 monolayers is a correlation-driven half semiconducting state. In this intriguing half semiconducting state — examples of which are rare — both the valence band maximum (VBM) and the conduction band minimum (CBM) are spin-polarized, and their spin orientations are identical. Moreover, the spin sign of the CBM in VS_2 is found to switch under moderate strain, undergoing a phase transition from a half semiconductor to a magnetic semiconductor. This opens up intriguing

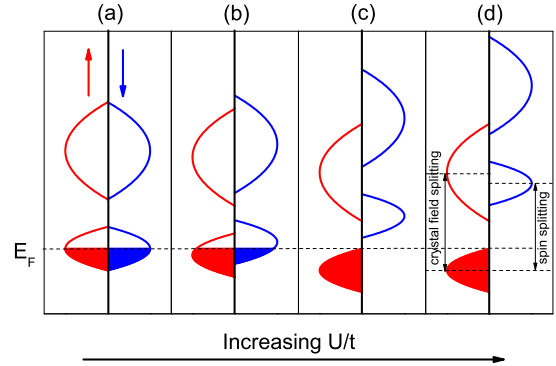


FIG. 1: (Color online) Energy band diagrams for trigonal-prismatic group-V MX_2 monolayers with increasing spin splitting of valence band. Depending on U/t , four different mean-field phases are expected: (a) nonmagnetic metal, (b) magnetic metal, (c) magnetic semiconductor, and (d) half semiconductor.

possibilities for applications in novel spin based electronics. Our analysis of other Group-V MX_2 monolayers ($M=V, Nb, Ta$; $X=S, Se, Te$) reveals a broad range of correlation-driven phases such as ferromagnetic metallic, ferromagnetic semiconducting states, and half semiconducting states (Fig. 1). We demonstrate that this rich phase diagram — interesting both from a fundamental as well as an applied perspective — has an intuitive interpretation in terms of localization of d electrons.

A trigonal-prismatic MX_2 monolayer is composed of one triangular transition-metal sublattice sandwiched between two sheets of chalcogen atoms. Chalcogen atoms are below and above the centers of metal triangles, resulting in a six-fold trigonal-prismatic coordination for the metal, cf. Fig. 2. The coordination splits the

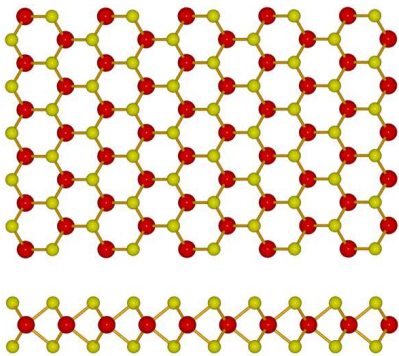


FIG. 2: (Color online) Top view and side view of trigonal-prismatic MX_2 monolayers. (M atoms in red and X atoms in yellow).

metal d orbitals into A'_1 (d_{z^2}), E' ($d_{xy}, d_{x^2-y^2}$), and E'' (d_{xz}, d_{yz}) manifolds [15]. Governed by the overlap with chalcogen orbitals, their mean energies lie in ascending order of A'_1 , E' , and E'' . The d_{z^2} , d_{xy} , and $d_{x^2-y^2}$ orbitals further hybridize with each other owing to common reflection symmetry, contributing a narrow valence subband and a wider conduction subband [16, 17]. In other words, the low energy bands of MX_2 are dominated by the onsite hybrid and the inter-site overlap of the d_{z^2} , d_{xy} , and $d_{x^2-y^2}$ orbitals of the 2D metal sublattice. A tight-binding model taking into account these three orbitals already captures well the dispersion of the low energy bands — especially the valence band [18]. Also recent experimental investigations provide evidence for the metal-metal interactions to define the electronic structure of such 2D systems [12]. For these reasons, a multi-orbital Hubbard model on the triangular lattice is a good candidate for describing the strongly correlated physics of d^1 MX_2 monolayers. However, to gain a qualitative understanding of the emergence of the various correlation-driven phases shown in the schematic diagrams of Fig. 1, we use a simpler, single band Hubbard model:

$$H = -t \sum_{i,j,\sigma} (c_{i\sigma}^\dagger c_{j\sigma} + c_{j\sigma}^\dagger c_{i\sigma}) + U \sum_i n_{i\uparrow} n_{i\downarrow}. \quad (1)$$

Here, t is the nearest-neighbor hopping integral, and U is the on-site coulomb potential. $c_{i\sigma}^\dagger$ ($c_{i\sigma}$) creates (annihilates) an electron of spin σ at site i , and $n_{i\sigma}$ is the number operator for spin σ at site i . U and t are two competing parameters that parametrize the localization and the mobility of the strongly correlated electrons, respectively. The onsite repulsion U is responsible for the spin splitting of the narrow d band. As illustrated in Fig. 1, on a mean-field level, there are four possible band structure configurations, depending on the magnitude of the spin splitting. Without any spin splitting (Fig. 1 a) the system is a half-filled nonmagnetic metal. In the second case (Fig. 1b) the two spin components of the

TABLE I: Electronic states for trigonal-prismatic MX_2 ($M=\text{V}, \text{Nb}, \text{Ta}$; $X=\text{S}, \text{Se}, \text{Te}$) computed at the level of hybrid functional DFT. *Although VSe_2 and VTe_2 are magnetic semiconductors, their VBM and CBM arise from splitting of different bands, similar to half semiconductors, unlike Fig. 1c.

| Composition | V | Nb | Ta |
|-------------|-----|----|----|
| S | HS | MM | MM |
| Se | MS* | MS | MS |
| Te | MS* | MS | MS |

narrow d band are partially separated and the system is a magnetic metal. As the spin splitting starts exceeding the bandwidth, such that the two spin components are fully separated (Fig. 1c), a magnetic semiconductor results. Finally, when the spin splitting of the narrow d band becomes larger even than the crystal field splitting, so that one spin component of the narrow d band is above the CBM, which is typically about 1.0 eV higher than the VBM for TMDCs, the system is a half semiconductor (Fig. 1d): both the VBM and the CBM are spin-polarized and have the same spin orientation. The first three states are frequently reported while the fourth one is rare in nature. Interestingly, as our calculations show, d^1 TMDCs span the entire gamut of phases shown in Fig. 1, including the half semiconducting state, which we predict to exist in VS_2 . We note that a large spin splitting comparable to the crystal field splitting does not always result in a half semiconductor: the VBM and CBM originating from two different spin-split bands may end up having different spins (as in the case of VSe_2 and VTe_2 ; see below).

We make the above predictions for the electronic structures of trigonal-prismatic MX_2 ($M=\text{V}, \text{Nb}, \text{Ta}$; $X=\text{S}, \text{Se}, \text{Te}$) monolayers based on first-principles calculations. (We note that although for VSe_2 and VTe_2 the trigonal-prismatic configuration is not the ground state, we investigate it here for its theoretical interest.) The calculations are performed using density functional theory as implemented in the Vienna ab initio simulation package (VASP) [19]. The exchange-correlation functional is considered at the level of the generalized gradient approximation (GGA) [20]. The screened hybrid functional method proposed by Heyd, Scuseria, and Ernzerhof (HSE) [21] is used. The single-particle equations are solved using the projector-augmented wave (PAW) method [22, 23] with a plane-wave basis and a cutoff energy of 500 eV. All the calculations are carried out in a slab model with the primary surface cell without considering any CDW distortion, since we focus on the electron-electron interaction only. Our results are summarized in Table I. While all three VX_2 ($X=\text{S}, \text{Se}, \text{and Te}$) materials show large spin splitting comparable to the crystal field splitting, only VS_2 has the same spin orientation for both CBM and VBM, and, therefore, is a half semi-

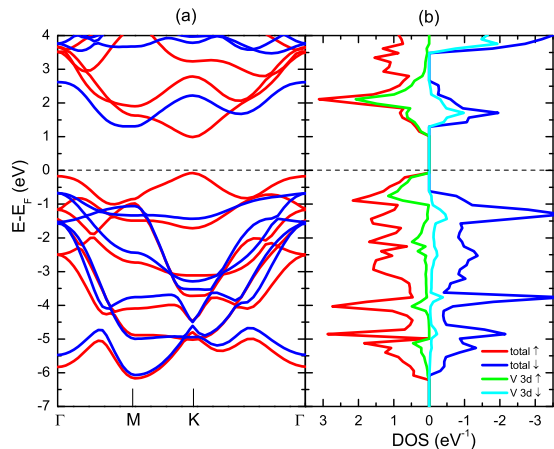


FIG. 3: (Color online) Spin-resolved (a) band structures and (b) density of states for VS_2 computed with hybrid DFT. The presented V $3d$ density of states are contributed by d_{z^2} , d_{xy} , and $d_{x^2-y^2}$ orbitals.

conductor. In trigonal-prismatic VSe_2 and VTe_2 they have different spin orientations (see Supplementary materials). Like NbSe_2 , NbTe_2 , TaSe_2 , and TaTe_2 they are thus ferromagnetic semiconductors, while NbS_2 and TaS_2 are ferromagnetic metals.

Half semiconducting state and direct band gap in VS_2 . According to our total energy calculations, the VS_2 monolayer is in a ferromagnetic ground state, consistent with both prior calculations [24] and experimental observations [25, 26]. The ferromagnetic state is more stable than both the nonmagnetic and the antiferromagnetic states (spins of nearest neighbors are opposite), by 367 meV and 689 meV, per cell, respectively. The magnetic moment per unit cell is calculated to be $1.0 \mu_B$. Each V atom contributes $1.30 \mu_B$, while each S atom contributes $-0.15 \mu_B$. As is seen from Fig. 3, the electrons near both the VBM and the CBM have the same spin orientation, making VS_2 monolayers moreover half semiconductors. The highest valence subband is made up of spin-up hybrid states of d_{z^2} , d_{xy} , and $d_{x^2-y^2}$. The Coulomb interaction causes a ~ 2.5 eV spin splitting, pushing the down-spin counterpart of this band into the conduction band. The CBM consists of spin-up electronic states of the higher hybrid band. As a result, the total density of states matches well the half semiconducting state illustrated by the schematic Fig. 1d. In addition, both the VBM and CBM are located at the K point, with a direct band gap of ~ 1.1 eV. The highest occupied state at K is 93 meV higher than the one at the Γ point. The lowest unoccupied state at K is 316 meV lower than that of the opposite spin at a local minimum near M . The direct band gap of the VS_2 monolayer is similar in magnitude to that of the isostructure MoS_2 monolayer, and it is well in the region of the visible spectrum — of great interest

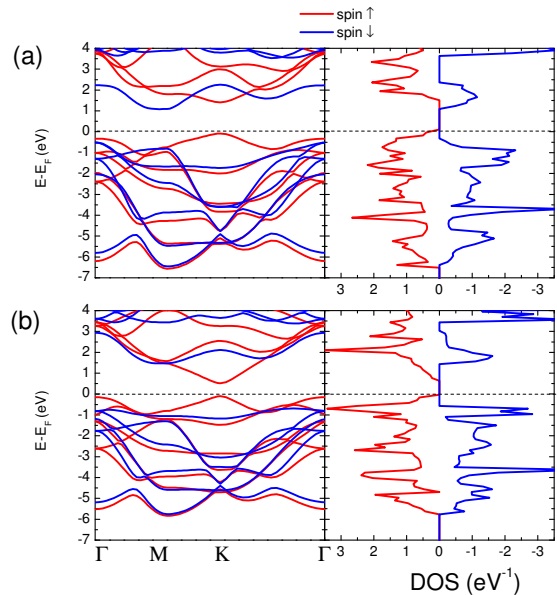


FIG. 4: (Color online) Spin-resolved electronic structures for (a) 3% contracted and (b) 3% expanded VS_2 .

for optoelectronic applications. We arrive at similar conclusions by performing additional, GGA+U calculations (see Supplementary materials).

Experimentally, VS_2 monolayers have not yet been realized. So far only thin films of VS_2 have been reported [27]. They are metallic, as a result of being in the octahedral phase and because of the interlayer interaction [28]. Further experimental efforts are needed to confirm the intriguing properties we predict for VS_2 monolayers.

Strain induced phase transition in VS_2 monolayer. Mechanical strain provides a means to tune the electronic structure of 2D electronic systems by controlling the spacing between atoms. We, therefore, next examine the effect of strain on the electronic structure of VS_2 . According to our calculations, compressive strain tends to decrease the energy of the half semiconducting state and destroy it while tensile strain tends to stabilize it. Fig. 4 shows the band structure and density of states of a VS_2 monolayer under 3% strain, i.e. the lattice constant was contracted or expanded by 3%. Under compressive strain, the atomic spacing of V atoms decreases. This increases the orbital overlap and hence the hopping integrals t of the d electrons. As a result, the width of the narrow d band is increased owing to the electron delocalization and the spin splitting is reduced. The system transitions into the normal ferromagnetic semiconducting state due to the lowering of the energy of the down spin counterpart of the valence d band (Fig. 4a). The lowest unoccupied state then is a down spin state near M , which has energy 327 meV lower than the lowest state at K , which is spin-up. According to our calculations, the critical strain for this transition is 2%. This is

a quite moderate, experimentally achievable value. On the other hand, tensile strain enlarges the atomic spacing and enhances the localization of the metal d electrons at the lattice sites. That localization in turn leads to a larger onsite interaction, which enlarges the energy splitting between opposite spins. Consequently, the half semiconducting state is enhanced as the down spin counterpart of the valence subband is lifted deeper into the conduction band (Fig. 4b). Our results reveal that the spin splitting of the d electronic states in VS_2 is sensitive to the atomic spacing of V atoms owing to electron localization. Thus, the spin sign of the conduction band can be switched by moderate, compressive strain. This phenomenon has direct application in spin-based electronics.

Electronic phases of group-V MX_2 monolayers. While VSe_2 and VTe_2 have similar spin splitting as VS_2 , pushing the down spin counterpart of the d valence subband into the conduction band, the VBM in those cases is not located in the spin-up d subband, but in a spin-split subband arising from deeper p bands. The VBM and CBM thus have different spin signs (see Supplementary materials), such that these materials are unconventional ferromagnetic semiconductors. On the other hand, NbS_2 and TaS_2 are ferromagnetic metals, and NbSe_2 , NbTe_2 , TaSe_2 , and TaTe_2 are normal ferromagnetic semiconductors. This series spans the entire range of strongly correlated phases illustrated in Fig.1. A summary of the phases is given in Table I.

There is a trend for small metal and large chalcogen components to stabilize the phase on the large U/t side of our Hubbard mean-field schematic Fig. 1, which can be attributed to electron localization. Consider MX_2 of the same metal but different chalcogen components X. In this case, the orbital properties of the metal components are fixed parameters, while the hopping integral is determined by the distance between the transition metal atoms. As shown in Fig. 5a, the ratio of metal diameter to the cell constant, d_M/a , decreases with increasing chalcogen radius from S to Te. Since this ratio qualitatively measures the overlap of the d orbitals, this results in a narrowing of the d band and an increase of the onsite interaction, i.e. a larger spin splitting. The phase variation and the trend of the energy gain by ferromagnetic order, $\Delta E = E_{FM} - E_{NM}$ (Fig. 5b) for MX_2 with different chalcogen components can be understood by these simple considerations. If one considers instead different metal components keeping the chalcogen component fixed, one can draw a similar conclusion (see Supplementary materials).

The above results provide strong evidence for the strongly correlated nature of electronic states in group-V TMDCs. So it is not surprising that contradicting predictions exist in the literature. Based on the GGA method, Pan recently reported that VX_2 monolayers are all semimetallic and ferromagnetic [29]. Wasey et al. predict VS_2 to be a semimetal, and VSe_2 and VTe_2 to

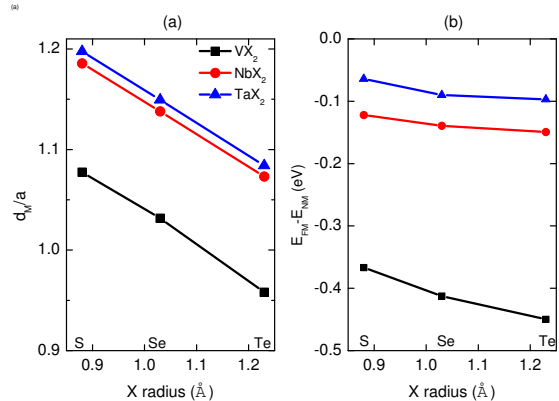


FIG. 5: (Color online) (a) The ratio of M diameter to the cell constant, d_M/a , and (b) the difference between the energies E_{FM} of the ferromagnetic and E_{NM} of the nonmagnetic states as a function of X radius for MX_2 . (M=V, Nb, Ta; X=S, Se, Te.).

be semiconductors with indirect band gaps [30]. Li et al. also predicted a semiconducting state for VSe_2 [31]. These variations in the results can be addressed by asking the following question: are the opposite spin components of the narrow d band in contact or fully separated? It is hard to give a conclusive answer at the level of the GGA method since the calculated band structure is close to the transition between the two. Our calculations based on the hybrid functional clearly demonstrate the existence of the half semiconducting state.

It should be noted that the predicted correlation driven ferromagnetic and insulating states are hard to observe in experiments as they are easily corrupted by doping or disorder [32–34]. The ferromagnetic, semiconducting state is based on a correlation-driven electronic configuration where the down spin component of the highest valence subband is a few eV higher than its up-spin counterpart and unoccupied. The energy gain over the nonmagnetic and metallic states from the spin exchange, however, is only a hundred meV or smaller. Occupation of the down-spin band would thus be energetically unfavorable, and doping collapses the system into the nonmagnetic and metallic state. Especially for NbX_2 and TaX_2 the stabilization energy for ferromagnetic order and the semiconducting state is on the order of only tens of meV, making these states likely too fragile to be observed. However, it is possible for the ferromagnetic and semiconducting states to survive in VX_2 since they have relatively large stabilization energies on the order of a hundred meV. This may explain why ferromagnetism has been observed in VS_2 multilayers.

In summary, we predict that the electronic states of d^1 TMDC monolayers span a rich variety of correlation-driven phases including magnetic metal, magnetic semiconductor, and half semiconductor. Our predictions are

based on hybrid functional DFT calculations. Most importantly, our calculations demonstrate that the VS₂ monolayer is a direct band gap half semiconductor, the electron spin orientation of which can be switched by moderate strain. Such easily tunable phase transitions are highly desirable and hold great promise for applications in spintronics. Our study moreover reveals the importance of the role of electron localization in the electronic structure of d¹ TMDCs, which is of fundamental interest in the theoretical understanding of these materials. We anticipate our findings to inspire further experimental and theoretical work, particularly with a view to application in novel electronics.

This work was supported by National Natural Science Foundation of China (Grant No. 61366007 and No. 11164032 and No. 61066005), Program for New Century Excellent Talents in University (Grant No. NCET-12-1080), Applied Basic Research Foundation of Yunnan Province (Grant No. 2011CI003 and No. 2013FB007), Program for Excellent Young Talents in Yunnan University and by the NSF under grant DMR-1055799 (M. K. and H. K. P.).

Note added: Shortly before completion of this manuscript we became aware of complementary work on VS₂, which confirms that the trigonal prismatic phase of the material studied here is indeed the ground state at the magnitude of strain considered here [35].

- [18] G.-B. Liu, W.-Y. Shan, Y. Yao, W. Yao, and D. Xiao, Phys. Rev. B **88**, 085433 (2013).
- [19] G. Kresse and J. Furthmüller, Phys. Rev. B **54**, 11 169 (1996).
- [20] J. P. Perdew, K. Burke, and M. Ernzerhof, Phys. Rev. Lett. **77**, 3865 (1996).
- [21] J. Heyd, G. E. Scuseria, and M. Ernzerhof, J. Chem. Phys. **118**, 8207 (2003); **124**, 219 906 (2006).
- [22] G. Kresse and D. Joubert, Phys. Rev. B **59**, 1758 (1999).
- [23] P. E. Blöchl, Phys. Rev. B **50**, 17953 (1994).
- [24] Y. Ma, Y. Dai, M. Guo, C. Niu, Y. Zhu, and B. Huang, ACS Nano **6**, 1695 (2012).
- [25] D. Gao, Q. Xue, X. Mao, W. Wang, Q. Xu, and D. Xue, J. Mater. Chem. C **1**, 5909 (2013).
- [26] M. Zhong, Y. Li, Q. Xia, X. Meng, F. Wu, and J. Li, Mater. Lett. **124**, 282 (2014).
- [27] J. Feng *et al.*, J. Am. Chem. Soc. **133**, 17832 (2011).
- [28] P. Darancet, A. J. Millis, and C. A. Marianetti, Phys. Rev. B **90**, 045134 (2014).
- [29] H. Pan, J. Phys. Chem. C **118**, 13248 (2014).
- [30] A. Wasey, S. Chakrabarty, and G. Das, arXiv:1408.1777 (2014).
- [31] F. Li, K. Tu, and Z. Chen, J. Phys. Chem. C **118**, 21264 (2014).
- [32] F. Zwick *et al.*, Phys. Rev. Lett. **81**, 1058 (1998).
- [33] F. Di Salvo, J. Wilson, B. Bagley, and J. Waszczak, Phys. Rev. B **12**, 2220 (1975).
- [34] H. Mutka, L. Zuppiroli, P. Molini, and J. Bourgoïn, Phys. Rev. B **23**, 5030 (1981).
- [35] M. Kan, B. Wang, Y. H. Lee, and Q. Sun, DOI: 10.1007/s12274-014-0626-5.

SUPPLEMENTARY MATERIALS

GGA+U calculations for VS₂. In addition to hybrid calculations, we also carried out GGA+U calculations to examine the effect of Hubbard U on the electronic structure of the VS₂ monolayer. According to our band structure calculations, the spin splitting of the narrow d band gradually when the onsite Coulomb potential U is increased from 0 to 4.0 eV (Fig. 6). The energy of the down spin component of the valence subband continually increases from that of its spin up counterpart until it is well above the CBM. As a result, the system undergoes a series of transitions, from semimetal to ferromagnetic semiconductor to half semiconductor, as proposed in Fig. 1. For a certain value of U (~ 3.5 eV), the GGA+U method results in the same prediction of a half semiconducting state as made by the HSE functional. The HSE functional includes some short range Hartree-Fock exchange, which partially cancels the self-interaction emerging in GGA and results in an increased localization of d electrons. The localization of electrons on atomic sites thus increases the onsite interaction. On the other hand, the GGA+U method imposes an extra onsite interaction, leading to larger spin splitting. The consistency of the two approaches demonstrates the critical role of correlation due to localization in the electronic

* Electronic address: yhe@ynu.edu.cn

- [1] B. Radisavljevic, A. Radenovic, J. Brivio, V. Giacometti, and A. Kis, Nat. Nanotechnol. **6**, 147 (2011).
- [2] Q. H. Wang, K. Kalantar-Zadeh, A. Kis, J. N. Coleman, and M. S. Strano, Nat. Nanotechnol. **7**, 699 (2012).
- [3] Z. Yin *et al.*, ACS Nano **6**, 74 (2011).
- [4] K. F. Mak, C. Lee, J. Hone, J. Shan, and T. F. Heinz, Phys. Rev. Lett. **105**, 136805 (2010).
- [5] K. F. Mak, K. He, J. Shan, and T. F. Heinz, Nat. Nanotechnol. **7**, 494 (2012).
- [6] H. Zeng, J. Dai, W. Yao, D. Xiao, and X. Cui, Nat. Nanotechnol. **7**, 490 (2012).
- [7] A. M. Jones *et al.*, Nat. Nanotechnol. **8**, 634 (2013).
- [8] D. Xiao, G.-B. Liu, W. Feng, X. Xu, and W. Yao, Phys. Rev. Lett. **108**, 196802 (2012).
- [9] X. Xu, W. Yao, D. Xiao, and T. F. Heinz, Nat. Phys. **10**, 343 (2014).
- [10] D. Shen *et al.*, Phys. Rev. Lett. **99**, 216404 (2007).
- [11] F. Weber *et al.*, Phys. Rev. Lett. **107**, 107403 (2011).
- [12] C. D. Malliakas and M. G. Kanatzidis, J. Am. Chem. Soc. **135**, 1719 (2013).
- [13] J. A. Wilson, F. Di Salvo, and S. Mahajan, Adv. Phys. **24**, 117 (1975).
- [14] B. Sipos, *et al.*, Nat. Mater. **7**, 960 (2008).
- [15] R. Huisman, R. De Jonge, C. Haas, and F. Jellinek, J. Solid State Chem. **3**, 56 (1971).
- [16] L. Mattheiss, Phys. Rev. B **8**, 3719 (1973).
- [17] R. Coehoorn, C. Haas, J. Dijkstra, C. Flipse, R. De Groot, and A. Wold, Phys. Rev. B **35**, 6195 (1987).

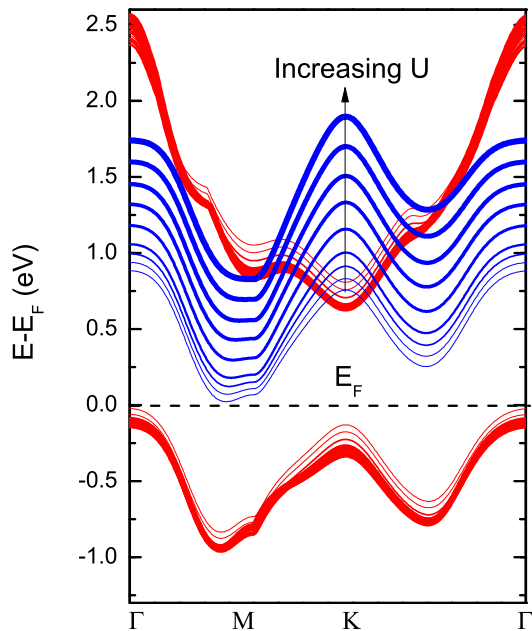


FIG. 6: The low energy band structure of VS_2 as a function of U between 0 and 4.0 eV (0.5 eV per step). The thickness of the line indicates the value of U .

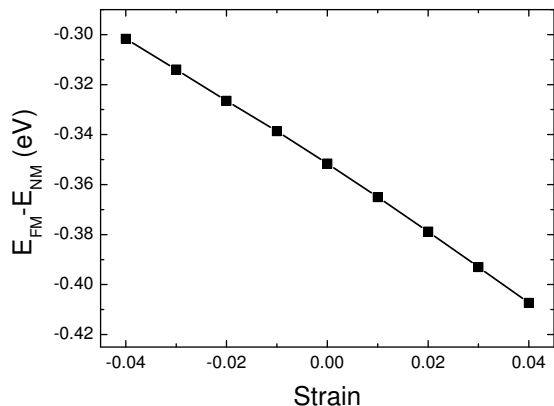


FIG. 7: Energy difference between the ferromagnetic and non-magnetic states of monolayer VS_2 as a function of strain.

structure of MX_2 .

Strain and ferromagnetic ordering. In Fig. 7, we show the energy gain of ferromagnetic order versus the non-magnetic states $E_{FM} - E_{NM}$ as a function of in-plane strain for monolayer VS_2 . As the strain varies from -4% (compressive) to 4% (tensile), the energy gain increases almost linearly from 0.30 eV to 0.41 eV. This demonstrates explicitly that compressive strain decreases the energy gain of ferromagnetic order and tends to destroy the half semiconducting state. On the other hand, tensile strain tends to enhance ferromagnetic ordering and hence the half semiconducting state.

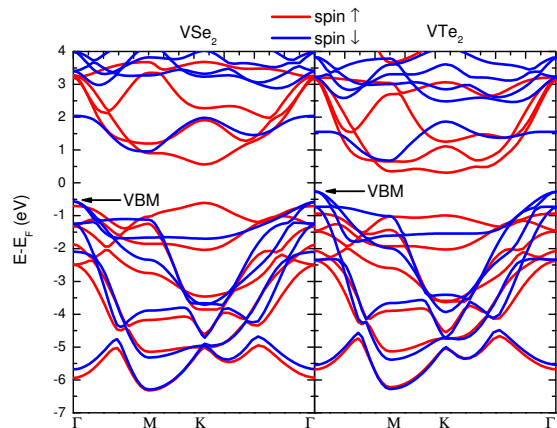


FIG. 8: Spin-resolved band structures for monolayer VSe_2 and VTe_2 .

Unconventional magnetic semiconductors, VSe_2 and VTe_2 . In Fig. 8, we show the spin-resolved band structures for trigonal-prismatic, monolayer VSe_2 and VTe_2 , respectively. The down spin counter part of the valence d band is above the CBM in these two compounds. However, in both cases, the VBM is not located in the up spin d band, but in a spin split subband arising from deeper p bands. Therefore, VSe_2 and VTe_2 are unconventional magnetic semiconductors which differ from both half semiconductors like VS_2 and magnetic semiconductors like $NbSe_2$, $NbTe_2$, $TaSe_2$, and $TaTe_2$. For VSe_2 , the VBM, made up of p bands, is only 40 meV higher than the highest d states at K . It may be possible to tune it into a half semiconducting state. However, for VTe_2 , the VBM is 731 meV higher, deviating greatly from a half semiconducting state.

Effect of metal atoms on localization and ferromagnetic ordering. The phases in Table I can be understood in terms of electronic localization on the metal atoms. In the main text we have shown how the different phases for the same metal atom with different chalcogen atoms can be understood within this picture. Here we consider the phase differences among MX_2 materials with the same chalcogen atom, but different metal atoms. The diameters of the group-V transition elements, V (3d), Nb (4d), and Ta (5d), are 3.42, 3.96, and 4.00 Å, respectively. According to our calculation, the cell constants for their compounds with sodium, for example, are 3.17, 3.35, and 3.35 Å respectively. As a result, the d_M/a ratio for VS_2 (1.08) is much smaller than for NbS_2 (1.19) and TaS_2 (1.20). Similar considerations apply for monolayers with Se or Te components. These comparisons show that the d electrons in VX_2 are more localized than those in NbX_2 and TaX_2 . Consequently, all VX_2 monolayers are well stabilized in the semiconducting state, while NbX_2 and TaX_2 fall into the critical region of metal to insulator transition. Also, the stabilization energy of ferromag-

netic order for VS_2 , ΔE , is 367 meV, much larger than those of NbS_2 (122 meV) and TaS_2 (64 meV), and it follows the same trend: the spin splitting in VS_2 is larger

than that in NbS_2 and TaS_2 owing to stronger electronic localization.